TRITA-EPP-90-04

# COMPLEMENTARY ASPECTS ON MATTER-ANTIMATTER BOUNDARY LAYERS

B. Lehnert

TRITA-EPP-90-04

# COMPLEMENTARY ASPECTS ON MATTER-ANTIMATTER BOUNDARY LAYERS

B. Lehnert

Stockholm, May 1990

Department of Plasma Physics and
Fusion Research
Royal Institute of Technology
S-100 44 Stockholm, Sweden

# COMPLEMENTARY ASPECTS ON MATTER-ANTIMATTER BOUNDARY LAYERS

B. Lehnert
Royal Institute of Technology, S-10044 Stockholm, Sweden

## ABSTRACT

This paper gives some complementary aspects on the problems of the matter-antimatter metagalaxy model and its cellular structure, as being proposed by Klein and Alfvén.

A previously outlined one-dimensional model of a magnetized matter-antimatter boundary layer is updated and extended, by introducing amended nuclear annihilation data, and by making improved approximations of the layer structure and its dependence on relevant parameters.

The critical beta value obtained from this model leads to critical plasma densities which are not high enough to become reconcilable with a cellular matter-antimatter structure within the volume of a galaxy. Additional investigations are required on the questions whether the obtained beta limit would still apply to cells of the size of a galaxy, and whether large modifications of this limit could result from further refinements of the theory and from the transition to a three-dimensional model.

Attention is called to the wide area of further research on ambiplasma physics, and on a three-dimensional cell structure with associated problems of equilibrium and stability. In particular, the high-energy ambiplasma component has to be further analysed in terms of kinetic theory, on account of the large Larmor radii of the corresponding electrons and positrons.

## 1. Introduction

Nearly four decades ago Klein [1-6] put forward a theory on the development of the metagalaxy, being symmetric with respect to the contents of matter and antimatter. This approach was further developed by Alfvén and Klein [7-10] who stressed that, during the present state of the metagalaxy, there must exist a cellular structure consisting of subregions which contain matter or antimatter and are separated by thin sheaths. In some respects the sheaths may be considered analogous to "Leidenfrost layers".

Consequently, such sheaths become a crucial part of the theory on a matter-antimatter universe. It was suggested that the sheaths should contain energetic particles which are created by annihilation reactions. However, on account of the large mean free paths at cosmical particle densities, there are difficulties in maintaining such layers and keeping apart the matter and antimatter cells, unless some special mechanism can be found which preserves the cellular structure.

Since the universe mainly consists of plasma, one such mechanism can be provided by a confining magnetic field, thereby leading to an ambiplasma boundary layer structure as outlined in Fig. 1 [11-13]. The problems of mater-antimatter boundary layers have many features in common with those of magnetic confinement in the research on controlled thermonuclear fuson. In particular, this applies to a model of cold-mantle systems where a plasma is separated from neutral gas by a magnetized partially ionized plasma boundary layer [14].

In this paper a number of complementary aspects will be added to the earlier investigations [11-13] on a one-dimensional matter-antimatter boundary layer model. These aspects include some modifications due to amended data on the annihilation processes and refinements in the description of the profile structure, as well as the identification of areas for further research on the transition from a one-dimensional to a three-dimensional model and its consequences for ambiplasma stability.

## 2. Data on the Annihilation Processes

The positron-electron ($e^+e^-$) annihilation in flight gives rise to two photons. For the low-energy components of the boundary layer model the annihilation takes place at non-relativistic velocities of impact, and for the high-energy component the corresponding velocities are relativistic. In the case of the low-energy component an increase in temperature from $T = 10^2K$ to $10^6K$ yields an annihilation reaction rate in the range from $\alpha_e \simeq 1.6 \times 10^{-18}$ to $8.5 \times 10^{-21}m^3/s$, as obtained from known data on the corresponding cross-section [8]. For the high-energy component a temperature $\hat{T}$ in the range $10^8 < \hat{T} < 10^{10}K$ yields an annihilation reaction rate $\hat{\alpha}_e \simeq 10^{-20}m^3/s$.

The proton-antiproton ($p^+p^-$) annihilation in flight gives rise to a cascade process. The final result of this is the creation of $f_a \simeq 1.63$ positron-electron pairs with an average energy equivalent to $\phi_a = 92 \times 10^6V$ per particle. The corresponding reaction rate varies from $\alpha_i \simeq 1.7 \times 10^{-17}$ to $1.7 \times 10^{-20}m^3/s$ when the low-energy component temperature T increases from $T = 10^2K$ to $10^8K$ and estimates are made on the basis of available data [8]. Thus $\alpha_i\sqrt{T} \simeq 1.7 \times 10^{-16}m^3K^{1/2}/s$ in this temperature range.

The values of $\hat{\alpha}_e$ and $\alpha_i$ deviate from those given earlier [7] and being adopted in the earlier analysis [11] of the boundary layer.

## 3. Complementary Aspects on the One-Dimensional Layer Model

The earlier analysis on the one-dimensional matter-antimatter boundary layer model [11,12] is in this section extended on a number of specific points. We limit ourselves to a quasi-neutral ambiplasma for which the Debye distance is much shorter than the characteristic dimension $x_o$ of the boundary layer in Fig.1.

### 3.1. The Characteristic Width of the High-Energy Component Layer

According to the earlier outlined low-beta model of the boundary layer given in Fig.1, the characteristic layer thickness becomes [11]

$$x_o \simeq (12kk_\eta/\alpha_i\sqrt{T_o}B_o^2)^{1/2} \qquad (1)$$

where $k_\eta = \eta_o T_o^{3/2}$, $T_o$ is the temperature of the low-energy components at the centre $x=0$ of the boundary layer in Fig.1, and $\eta_o$ stands for the corresponding resistivity in the transverse direction of the magnetic field $B_o \equiv B(x=0)$. Here the possibility of anomalous effects discussed later in Section 4.3.1 is taken into account by introducing the form

$$k_\eta = c_a k_{\eta c} \qquad k_{\eta c} = 129(\ell n\Lambda) \qquad (2)$$

where $k_{\eta c}$ represents classical resistivity and $c_a$ is a factor due to anomalous transport of the low-energy component. Since $\alpha_i\sqrt{T_o}$ is nearly constant according to Section 2, the layer thickness of eq. (1) becomes $x_o \simeq 7.9 \times 10^{-2}\sqrt{c_a}/B_o$ in SI units which are used throughout this paper.

Moreover, the Larmor radius of the high-energy positrons and electrons becomes

$$\hat{a}_e = \phi_a / cB \tag{3}$$

Eqs. (1) and (3) combine to

$$\hat{a}_e / x_o = (\alpha_i \phi_a^2 \sqrt{T_o} / 12 k k_\eta c^2)^{1/2} \tag{4}$$

With the data given in Section 2, and putting $\ell n \Lambda = 50$, the result of eq. (4) becomes $\hat{a}_e / x_o \approx 3.9 / \sqrt{c_a}$.

The consequences of the result (4) are as follows:

- The value of $\alpha_i$ adopted in the earlier analysis [11] leads to ratios $\hat{a}_e / x_o$ being substantially smaller than unity, whereas the values of $\alpha_i$ given in Section 2 yield ratios $\hat{a}_e / x_o$ of the order of 4 when the transport of the low-energy component remains classical. In this case the high-energy component has to be treated in terms of kinetic theory when a length scale of the order of $x_o$ is being considered. It also implies that the earlier picture of the boundary layer given by Fig.1 has to be modified as outlined in Fig.2. The high-energy component thus obtains a density profile the half width $\hat{x}_o$ of which substantially exceeds the width $x_o$ and which is of the order of the Larmor radius $\hat{a}_e$ of eq. (3). In the first approximation we thus put $\hat{x}_o \approx \hat{a}_e \approx 4 x_o$. In the case of Fig.2, the low-energy component can still be treated in terms of a macroscopic fluid model, on a scale given by the layer thickness $x_o$ of eq. (1).

- If, on the other hand, the low-energy components become subject to anomalous transport and $c_a \gg 1$, a situation similar to that of Fig.1 is recovered, i.e. where $\hat{x}_o < x_o$ and $\hat{a}_e \ll x_o$.

3.2. The Diffusion of the High-Energy Components

The diffusion rate of the high-energy components can be crudely estimated by means of macroscopic fluid theory, for length scales which are comparable to or larger than $\hat{x}_o$. With a diffusion velocity $\hat{v}_d$ the corresponding diffusion time is of the order of

$$\hat{t}_d = \hat{x}_o/\hat{v}_d \simeq 6\sqrt{\hat{T}_o}\hat{x}_o^2/x_o^2\alpha_i\sqrt{T_o}\hat{n}_o \qquad (5)$$

where $\hat{n}_o = \hat{n}(x=0)$ and $\hat{T}_o = \hat{T}(x=0)$ are the density $\hat{n}$ and temperature $\hat{T}$ of these components at $x=0$. The diffusion time $\hat{t}_d$ has to be compared to the characteristic time

$$\hat{t}_\alpha = \hat{n}_o/(d\hat{n}_o/dt) = \hat{n}_o/\alpha_i n_o^2(\hat{x}_o/x_o)^2 \qquad (6)$$

for density increase of the high-energy components by annihilation of the low-energy components which have the density $n_o \equiv n(x=0)$. Combination of expressions (5) and (6) yields

$$\hat{t}_d/\hat{t}_\alpha \simeq 6(n_o/\hat{n}_o)^2(\hat{T}_o/T_o)^{1/2}(\hat{x}_o/x_o)^2 \qquad (7)$$

In the case $c_a = 1$ of classical diffusion where $\hat{x}_o \simeq 4x_o$ and when $\hat{n}_o$ is of the order of $n_o$, we then have $\hat{t}_d \gg \hat{t}_\alpha$ for $\hat{T}_o \gg T_o$ which confirms that diffusion of the high-energy component can be neglected in a first approximation [11]. This does on the other hand not hold in the case $c_a \gg 1$ of anomalous diffusion.

### 3.3. The Particle Balance of the High-Energy Components

For a negligible diffusion rate of the high-energy components it is now possible to generalize an earlier deduced relation between the high- and low-energy component densities. Thus, the high-energy component densities become

$$\hat{n}_e^{+-} = -\frac{1}{2}(n_e^{+-}+N) + \left[\frac{1}{4}(n_e^{+-}+N)^2 + f_a n_i^+ n_i^- (n_e^{+-}+N)\alpha_i/(n_e^{-+}+N)\hat{\alpha}_e\right]^{1/2} \quad (8)$$

in terms of the low-energy component densities $n_i^+$, $n_i^-$, $n_e^+$, $n_e^-$, where $f_a$ is the number of positron-electron pairs created per annihilation reaction,

$$N = (n_e^+ + n_e^-)\hat{\rho}/\alpha_e \quad (9)$$

and $\hat{\rho} = e^2 k_\eta / m_e \hat{T}^{3/2}$ is the rate of Coulomb impacts of the high-energy components. In particular, at the centre x=0 of the boundary layer in Figs.1 and 2 we have $n_i^+ \approx n_i^- \approx n_e^+ \approx n_e^- \equiv n_o$ and $\hat{n}_e^+ = \hat{n}_e^- \equiv \hat{n}_o$. At x=0 relation (8) then reduces to

$$\hat{n}_o/n_o \equiv f_o = -\frac{1}{2}(1+2\hat{\rho}_o/\alpha_e) + \left[\frac{1}{4}(1+2\hat{\rho}_o/\alpha_e)^2 + f_a f_\alpha\right]^{1/2} \quad (10)$$

where $f_\alpha = \alpha_i/\alpha_e$. This result applies even in the case $\hat{a}_e > x_o$.

### 3.4. The Diffusion of the Low-Energy Components

The diffusion of matter and antimatter towards the sink produced by annihilation reactions at the centre of the boundary layer in Fig.1 has been described in the earlier analysis. In a first crude approximation the parts of the low-energy

lensity listributions ranging from $x_o$ and far outwards into the pure matter or antimatter regions can be written as [11]

$$n_i^{+-}(x)/n_o = [1 \mp 4(x/x_o)(T_d/T_o)^{1/2}]^{-1/2} \quad (x\lessgtr \mp x_o) \tag{11}$$

Here $T_d$ stands for the temperature of the low-energy components at a distance from $x=0$ where the annihilation reactions can be neglected. Far away from the layer centre there is a temperature $T_\infty \equiv T(|x| \gg x_o)$ of the low-energy components which is expected to be much lower than $T_o \equiv T(x=0)$. The corresponding density gradient $dn_i^{+-}/dx$ at $|x| \gg x_o$ then also becomes small.Consequently, the density $n_\infty \equiv n_i^{+-}(|x| \gg x_o)$ can be approximated by the expression

$$n_o/n_\infty \equiv f_\infty = [1 + 4\nu_o]^{-1/2} \tag{12}$$

Here $\nu_o = x_d/x_o$ is defined by the distance $x_d$ from $x=0$ at which the low-energy components have a sufficiently high temperature $T_d$ to establish a noticeable density gradient of the diffusion process.

## 3.5. The Heat Balance of the High-Energy Components

Following the earlier analysis on the heat balance of the high-energy components [11], the corresponding temperature at $x=0$ can be written as

$$\hat{T}_o \simeq c_o/a_o \tag{13}$$

$$c_o = \alpha_i e\phi_a n_o^2 \tag{14}$$

$$a_o = \hat{n}_o[(3/2)k\hat{\alpha}_e(n_o + \hat{n}_o) + k_c B_o^2] \tag{15}$$

where $B_o \equiv B(x=0)$ and $k_c = 5.3 \times 10^{-24}$ stands for the synchrotron radiation loss. In expression (13) bremsstrahlung and energy transfer by Coulomb collisions have been neglected, as can be shown to be a good approximation within the parameter ranges of interest in this connection. Eqs. (13)-(15) are not particularly sensitive to the question whether or not a fluid model can be applied to the high-energy component.

### 3.6. An Estimation of the Low-Energy Component Temperature

A first estimation of the low-energy component temperature can be made by a simple order-of-magnitude deduction based on the heat balance equation. The heat source is due to heat being transferred from the high-energy component by Coulomb collisions. There are heat losses due to bremsstrahlung and synchrotron radiation. In addition, matter which is annihilated within the boundary layer is assumed to be replaced by matter which arrives from cold surrounding regions at distances $d \gg x_o$, thereby being ionized and heated in the region $-\hat{x}_o < x < \hat{x}_o$. The resulting heat balance equation can be approximated by the simple form

$$3k\hat{\rho}_o\hat{n}_o\hat{T}_o \simeq k_b n_\infty\sqrt{T_o} + k_c B_\infty^2 T_o + \\ + (3kT_o + W)(4kk_\eta n_\infty / B_\infty^2 x_o \hat{x}_o \sqrt{T_o}) \qquad (16)$$

where $k_b = 1.7 \times 10^{-40}$ VAm$^3$K$^{-1/2}$ and $k_c = 5.3 \times 10^{-24}$ Am$^4$/Vs$^2$K stand for bremsstrahlung and cyclotron radiation, $n_\infty$ and $B_\infty$ are the low-energy component density and the magnetic field strength at the distance $\hat{x}_o$ from the centre $x=0$ of the layer, and $W = 2.17 \times 10^{-18}$ J is the ionization energy of hydrogen. Eq. (16) is solved with respect to $T_o$ yielding

$$\sqrt{T_o} = -(c_b + c_n)/2c_c + \{[(c_b + c_n)/2c_c]^2 + (1/c_c)\}^{1/2} \qquad (17)$$

where

$$c_b = 2.3 \times 10^{-14} (\hat{T}_o)^{1/2} / f_o f_\infty \tag{18}$$

$$c_c = 7.0 \times 10^{2} (B_\infty^2 / f_o f_\infty n_\infty) (\hat{T}_o)^{1/2} \tag{19}$$

$$c_n = 7.9 \times 10^{-14} \quad (\hat{T}_o)^{1/2} \left[1 + (W/3kT_o)\right] / f_o f_\infty \tag{20}$$

## 3.7. The Beta Limit

On the basis of the results presented in Sections 3.1-3.5, a modified expression for the earlier deduced beta limit [12] will now be derived. As the pressure $\hat{p}_o = 2\hat{n}_o k\hat{T}_o$ of the high-energy components at $x=0$ is allowed gradually to increase, the magnetic field $B_o$ at the centre $x=0$ becomes weakened as compared to the field $B_\infty \equiv B(x = \pm\infty)$ far away from $x=0$. Consequently, this "pushes" out the magnetic field from the layer centre and deforms the boundary layer configuration as compared to a low-beta case. The corresponding pressure balance relation is given by

$$2\mu_o \hat{p}_o = B_\infty^2 - B_o^2 \equiv f_B B_\infty^2 \tag{21}$$

The earlier discussed equilibrium limit [12] corresponds to $f_B = 1$. Here we allow $f_B$ to adopt values being of the order of but smaller than unity. This corresponds to a high beta limit which could be due to the onset of an instability or some other mechanism which disrupts the layer before the ultimate limit $f_B = 1$ is being reached. A corresponding situation with a critical value of $f_B$ below unity could apply to the three-dimensional boundary layer geometry later discussed in Section 4 of this paper.

With these starting points combination of eqs. (21), (9) and (12)-(15) yields the condition

$$(B_\infty^2/n_\infty)_c = -g + (g^2 + h^2)^{1/2} \simeq h^2/2g \quad \text{for} \quad g \ll h \tag{22}$$

for the critical beta limit where

$$g = 3k\hat{\alpha}_e f_\infty (1 + f_o)/4k_c(1 - f_B) \tag{23}$$

$$h^2 = 4\mu_o k\alpha_i e\phi_a f_\infty^2/k_c f_B(1 - f_B) \tag{24}$$

and

$$h^2/2g = 8\mu_o e\phi_a \alpha_i f_\infty/3\hat{\alpha}_e f_B(1 + f_o) \tag{25}$$

## 3.8. Numerical Illustrations

The present deductions will now be illustrated by a number of examples as follows:

- The ratio $f_o = \hat{n}_o/n_o$ of the high- and low-energy density values at $x=0$ is shown in Fig.3 as a function of the high- and low-energy component temperatures $\hat{T}_o$ and $T_o$. The figure demonstrates that $f_o$ becomes a rather slow function of $\hat{T}_o$, but decreases when $T_o$ increases.

- The high-energy component temperature $\hat{T}_o$ is determined from the heat balance equation (13) of the same component. The variation of $\hat{T}_o$ with the low-energy component temperature $T_o$ is shown in Fig.4 at the fixed values $f_o = 4$, $f_\infty = 0.2$ and $B_\infty^2/n_\infty = 10^{-17}$. The decrease in $\hat{T}_o$ with increasing $T_o$ is mainly due to the fact that the reaction rate $\alpha_i$ decreases when $T_o$ increases.

- The low-energy component temperature is related to the high-energy component temperature by the crudely estimated relation (17) as shown in Fig.5 for $f_o = 4$, $f_\infty = 0.2$ and $B_\infty^2/n_\infty = 10^{-17}$. Figures 4 and 5 are consistent as far as orders of magnitude is concerned. The decrease in $T_o$ at increasing $\hat{T}_o$ is due to the fact that the heat transfer by Coulomb collisions decreases at increasing $\hat{T}_o$.

- The critical values $n_{\infty c}$ and $B_{\infty c}$ related by the beta limit of eq. (22) are demonstrated by Fig.6 for $f_o = 4$, $f_\infty = 0.2$ and $f_B = 0.5$. The obtained values of $n_{\infty o}$ are too low to apply to the more condensed regions of interstellar space within a galaxy where the average particle density is expected to be of the order of $10^6\ m^{-3}$ and the average magnetic field strength to be $10^{-10}$ to $10^{-9}$ tesla [7,8]. For interstellar regions of lower density, and for intergalactic space where Leidenfrost layers would separate galaxies from each other [8], condition (22) could possibly apply to relevant magnetic field strengths. However, this question, as well as the question of extrapolating condition (22) to a rigorous three-dimensional model, require further investigations.

## 4. Areas for Further Research

The so far performed analysis on a one-dimensional matter-antimatter boundary layer only represents a first crude approach to the present ambiplasma problems. In this section some areas for further research will be identified.

### 4.1. Ambiplasma Physics

Within the boundary layer of Fig.1 there is an ambiplasma the physics of which cannot be extrapolated in an easy manner from that of an ordinary matter plasma. In a rigorous theory of a magnetized ambiplasma there are new features which become included in the approaches based on fluid theory as well as on kinetic theory. Here the following can be mentioned:

- In a model with high- and low-energy components the ambiplasma has to be treated in terms of six particle species. This both introduces additional interaction effects between the species and increases the degrees of freedom for which the quasineutrality condition can be satisfied.

- Contrary to an ordinary plasma, there is symmetry in the ambiplasma components with respect to particle mass and charge. This leads to symmetric and more complicated forms of the MHD moment equations, such as those describing the particle, momentum and heat balance in a centre-of-mass system. In particular, there are positively and negatively charged particles having the same mass-to-charge ratios and Larmor radii, and being subject to inertia forces of the same magnitude.

- There are annihilation reactions included as particle and energy sources in the ambiplasma balance. This leads to high-energy components which have a substantially higher temperature than the low-energy components. In a more rigorous

approach the high-energy components have to be treated in terms of kinetic theory, and this could also introduce some modifications in the balance of the low-energy components.

It has to be further analysed how far the mesons from the $(p^+p^-)$ cascade process could move with respect to their point of creation, before this process has been completed.

## 4.2. The Extension to Three-Dimensional Geometry

A cosmical cellular ambiplasma model has necessarily to be three-dimensional. The simple pictures of Fig.1 and 2 only represent a first step in the analysis on the boundary layer problem. In an extension to three-dimensional geometry, the following points become important:

- A cellular structure has to be considered where matter and antimatter cells of various size form a three-dimensional pattern in which neighbouring cells are separated from each other by ambiplasma boundary layers in all directions of space.

- A magnetic confinement of the cell structure and its boundary layers has to be established. One possible scenario of each cell consists of a central region with closed electric currents which then produce a dipole-like confining magnetic field in the remote boundary regions of the cell.

- The magnetic confinement of the cell structure inevitably produces a complicated three-dimensional magnetic field geometry, thereby including magnetic separatrices, magnetic zero points (x-points), and magnetic zero lines. On the average the magnetic field of each cell becomes concave with respect to the interior of the cell.

- The magnetic field geometry and its curvature, the pressure gradients in the ambiplasma boundary layers, and a number of other features, raise the question of stability of the ambiplasma and its boundary layers.

## 4.3. The Stability Problem

There are a number of instability modes, being equivalent to those of an ordinary plasma, as well as other modes being specific of an ambiplasma, which could become crucial to the existence of the cellular structure. Here only some speculations can be presented on this rather extensive problem.

### 4.3.1. Instability Modes

In an ordinary plasma there is a number of MHD-like modes with comparatively short growth rates, by which a plasma equilibrium can be disrupted in a violent way. Similar modes have to be analysed in the present ambiplasma case. Among these the following can be mentioned:

- The pressure-gradient driven electrostatic flute-type instability is expected to arise under certain conditions of the three-dimensional magnetic field line curvature. even at low beta values.

- At high beta values the same field geometry sometimes gives rise to an electromagnetic ballooning-type instability by which the weakest parts of the magnetic field in the boundary layer can be pushed outwards by the ambiplasma pressure.

- Resistive modes have possibly to be considered for the low-energy components when these are at a sufficiently low temperature, in particular when electric currents are flowing along the magnetic field lines.

- Mirror instabilities are not unimaginable, in particular when these become enhanced by an increased local pressure through annihilation reactions. This would be the case when matter

slides towards a region between two magnetic mirrors, thereby enhancing the low-energy component density locally.

Also microscopic velocity space modes have to be taken into account, with their associated effects on anomalous plasma transport. From the analysis of an ordinary plasma, these modes are expected to be less violent and less destructive to the ambiplasma transport and confinement. Since the layer thickness $x_o$ of eq. (1) depends on the square root of the resistivity coefficient $k_\eta$, it is likely that even a rather strong anomalous transport can become acceptable, i.e. without leading to large modifications of the models in Fig.1 and 2.

### 4.3.2. Possible Existence of Stabilizing Mechanisms

When discussing the instability modes of the previous subsection, also a number of stabilizing effects have to be kept in mind:

- Not all configurations with a "wrong" field line curvature are necessarily MHD unstable. The stability condition depends among other things on the specific relations between the pressure and magnetic field distributions in coordinate space. Thus, there are cases of "maximum-average-B" flute stabilization which can also be reinforced by the presence of magnetic x-points and zero lines [15-17]. Further there is a beta limit of the ballooning modes.

- MHD-like finite Larmor radius (FLR) effects and fully kinetic large Larmor radius (LLR) effects can have a strong stabilizing influence on a number of modes, in particular at intermediate and high beta values.

- The high-energy components could provide a certain "rigidity" due to their high temperature, and this may in certain cases have a stabilizing influence on the low-energy component modes.

- The annihilation reactions could sometimes have a stabilizing influence on modes for which an expansion of the ambiplasma leads to a density decrease, with a corresponding decrease in the annihilation rate, and in the high-energy component temperature.

## 5. Conclusions

The results of this paper can be summarized as follows:

- An earlier outlined one-dimensional model on matter-antimatter boundary layers has been updated and extended, by introducing amended nuclear annihilation data and by making improved approximations for the layer structure and its parameters.

- The width $\hat{x}_o$ of the high-energy density profile is found to exceed the characteristic width $x_o$ of the low-energy density profile by a factor of about four in the case of classical transport. In the case of strongly enhanced anomalous transport of the low-energy components, it is on the other hand possible to reach a situation where $\hat{x}_o$ is smaller than $x_o$.

- The critical beta value of the present plane model leads to critical plasma densities which are not sufficiently high to become reconcilable with a cellular structure within the volume of galaxy. Further research is required on the questions whether the present results could apply to cells which separate galaxies from each other, and whether large modifications of the beta limit would result from the transition to a three-dimensional model.

- Attention is called to the wide area of further research which is required for a rigorous description of an ambiplasma, and for the analysis of a three-dimensional cellular

structure of a metagalaxy model. Thus, there are several basic features by which ambiplasma physics differs from the physics of an ordinary plasma, and there are a number of problems concerning ambiplasma stability in three-dimensional field geometry. Also the high-energy component has to be further analysed in terms of kinetic theory, on account of the large Larmor radii of its electrons and positrons.

## 6. Acknowledgements

The author is indebted to Prof. H. Alfvén and Drs. P. Carlquist and M. Jändel for valuable discussions on the problems treated in this paper.

Stockholm, May 30, 1990

## 7. References


[1] O. Klein, "Les processes nucléaires dans les astres", Societé Royale des Sciences, Liège (1953), pp. 42-51.

[2] O. Klein, "La structure et l'évolution de l'universe", Institut International de Physique Solvay, Bruxelles (1958), pp. 33-51.

[3] O. Klein, "Einige Probleme der allgemeinen Relativitätstheorie", in Werner Heisenberg und die Physik unserer Zeit, Braunschweig (1961), pp. 58-72.

[4] O. Klein, "Mach's Principle and Cosmology in their Relation to General Relativity", in Recent Developments in General Relativity, Pergamon Press, Oxford (1962), pp. 293-302.

[5] O. Klein, "Instead of Cosmology", Nature 211 (1966)1337-1341.

[6] O. Klein, "Arguments concerning relativity and cosmology", Science 171 (1971)339-345.

[7] H. Alfvén, "Antimatter and the Development of the Metagalaxy", Rev.Mod.Phys. 37(1965) 652-665.

[8] H. Alfvén, Cosmic Plasma, D. Reidel Publ.Comp., Dordrecht 1981, Ch. IV and VI.

[9] H. Alfvén, "Cosmology in the Plasma, Universe: An Introductory Exposition", IEEE Transactions on Plasma Science 18(1990) 5-10.

[10] H. Alfvén and O. Klein,"Matter-Antimatter Annihilation and Cosmology", Arkiv f.Fysik 23(1962)187-194.

[11] B. Lehnert, "Problems of Matter-Antimatter Boundary Layers", Astrophys. and Space Sci. 46(1977)61-71.

[12] B. Lehnert, "Beta Limitation of Matter-Antimatter Boundary Layers", Astrophys. and Space Sci. 140(1988)77-83.

[13] B. Lehnert, "Matter-Antimatter Boundary Layers with a Magnetic Neutral Sheet", Astrophys. and Space Sci. 53 (1978)459-465.

[14] B. Lehnert, "Screening of a High-Density Plasma from Neutral Gas Penetration", Nuclear Fusion 8 (1968)173-181.

[15] B. Lehnert, "Plasma Stability in an Inhomogeneous Magnetic Field", Phys. Fluids 5 (1962)432-438, and Dynamics of Charged Particles, North-Holland Amsterdam 1964, Ch.8.

[16] T. Hellsten, "Magnetohydrodynamic Stability of a Plasma Confined in a Convex Poloidal Magnetic Field", Royal Inst. of Technology, Stockholm, TRITA-EPP-76-18 (1976).

[17] B. Lehnert, "On the Stabilization of Flute-type Disturbances in a Magnetized Plasma", Physica Scripta 13(1976)317.

Figure Captions

Fig.1. Outline of the earlier deduced one-dimensional low-beta model describing a magnetized matter-antimatter boundary layer. The width $x_o$ is given by the combined diffusion-annihilation process of the low-energy components, and the width $\hat{x}_o$ refers to the density profile of the high-energy components. This picture applies to the case of anomalous diffusion of the low-energy component, thereby yielding an increased thickness $x_o > \hat{x}_o$.

Fig.2. Analogous to Fig.1 but applying to the case of classical diffusion of the low-energy component, thereby resulting in $x_o = \hat{x}_o/4$. In the figure $n$ and $\hat{n}$ refer to the density profiles of the low- and high-energy components, respectively.

Fig.3. Density ratio $f_o = \hat{n}_o/n_o$ at the centre of the boundary layer as a function of the low- and high-energy component temperatures $T_o$ and $\hat{T}_o$.

Fig.4. The high-energy component temperature $\hat{T}_o$ as determined from the heat balance of the same component. The diagram illustrates the case where $f_o = 4$, $f_\infty = 0.2$ and $B_\infty^2/n_\infty = 10^{-17}$.

Fig.5. The low-energy component temperature $T_o$ as estimated from the heat balance of the same component: The diagram illustrates the case $f_o = 4$, $f_\infty = 0.2$ and $B_\infty^2/n = 10^{-17}$.

Fig.6. The beta limit given by eq. (22) with $T_o$ as a parameter and $f_o = 4$, $f_\infty = 0.2$, $f_B = 0.5$.

Fig. 1

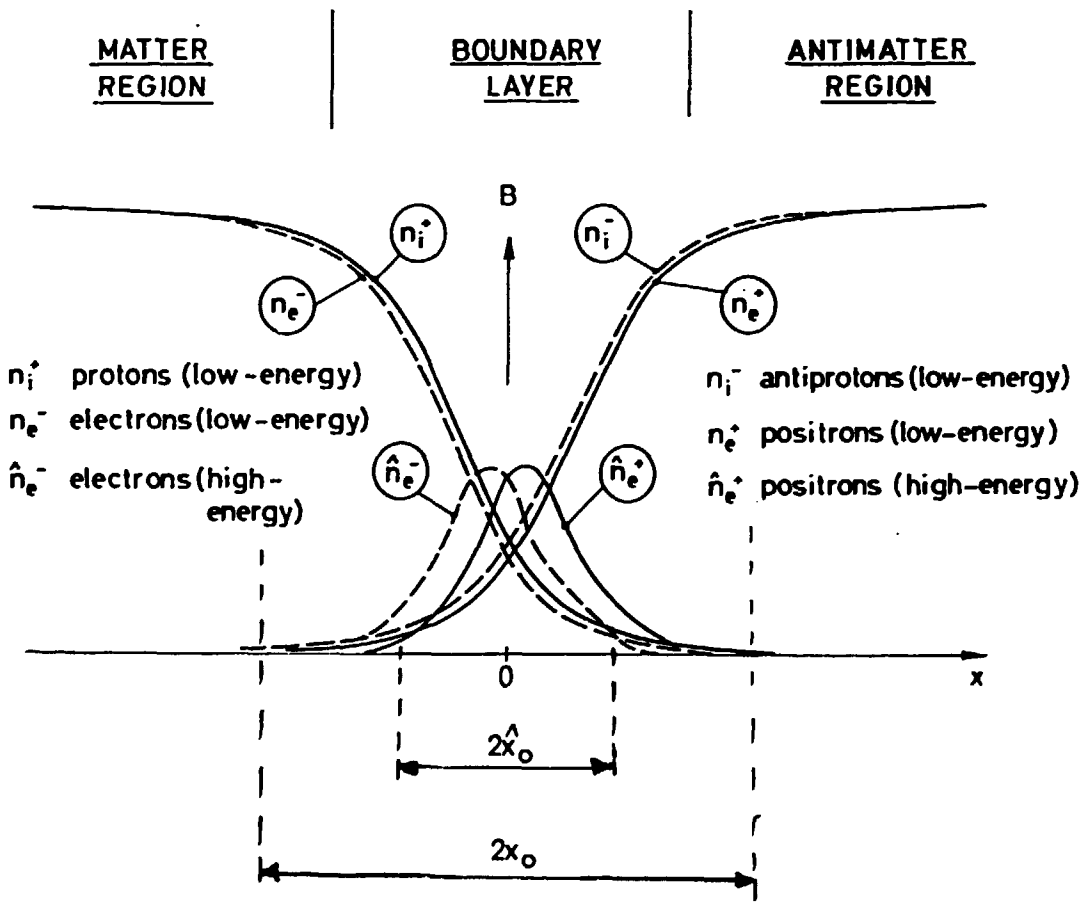
MATTER REGION
BOUNDARY LAYER
ANTIMATTER REGION
B
$n_i^+$
$n_e^-$
$n_i^-$
$n_e^+$
$n_i^+$ protons (low-energy)
$n_e^-$ electrons (low-energy)
$\hat{n}_e^-$ electrons (high-energy)
$n_i^-$ antiprotons (low-energy)
$n_e^+$ positrons (low-energy)
$\hat{n}_e^+$ positrons (high-energy)
$\hat{n}_e^-$
$\hat{n}_e^+$
0
x
$2\hat{x}_o$
$2x_o$

Fig. 2

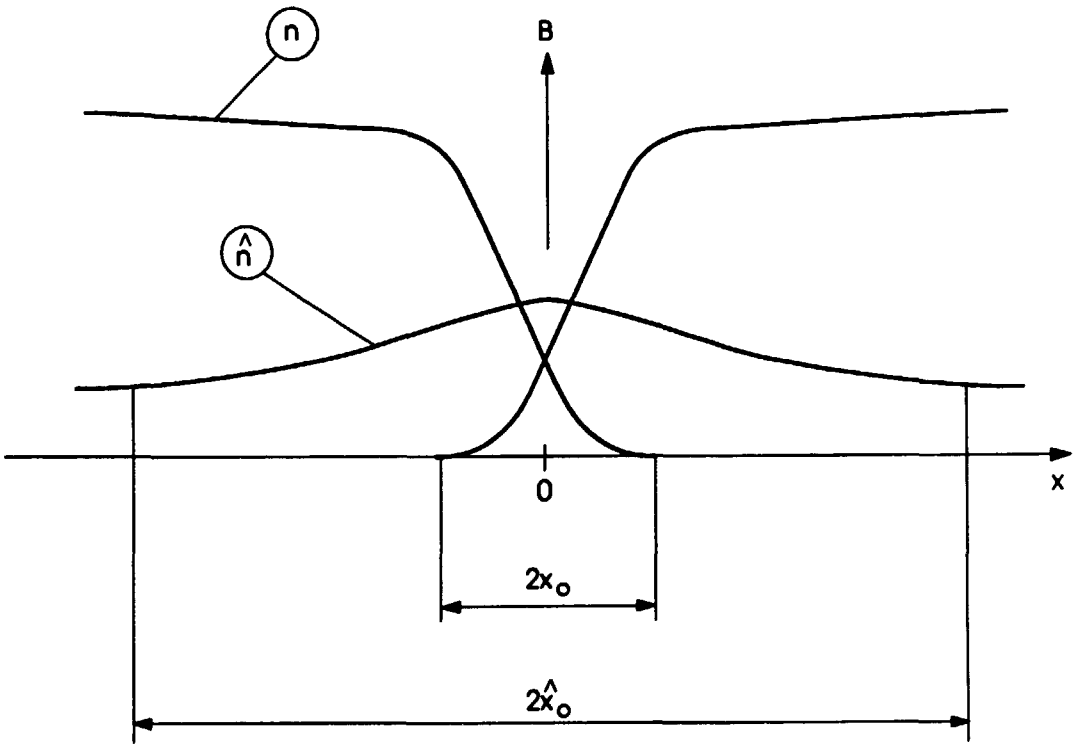

Fig 3

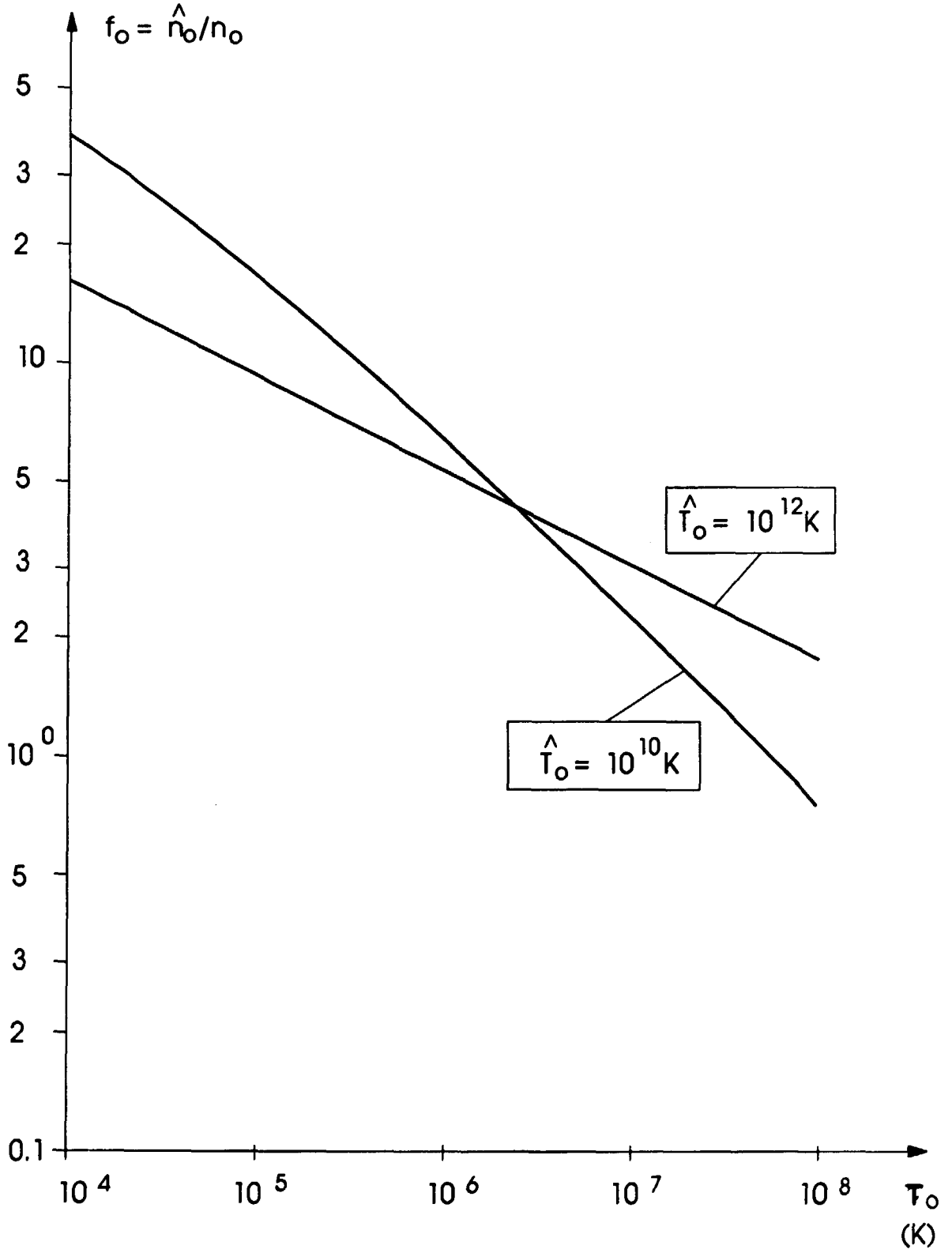
$f_o = \hat{n}_o/n_o$
5
3
2
10
5
3
2
$10^0$
5
3
2
0.1
$10^4$
$10^5$
$10^6$
$10^7$
$10^8$
$T_o$
(K)
$\hat{T}_o = 10^{12}K$
$\hat{T}_o = 10^{10}K$

Fig. 4

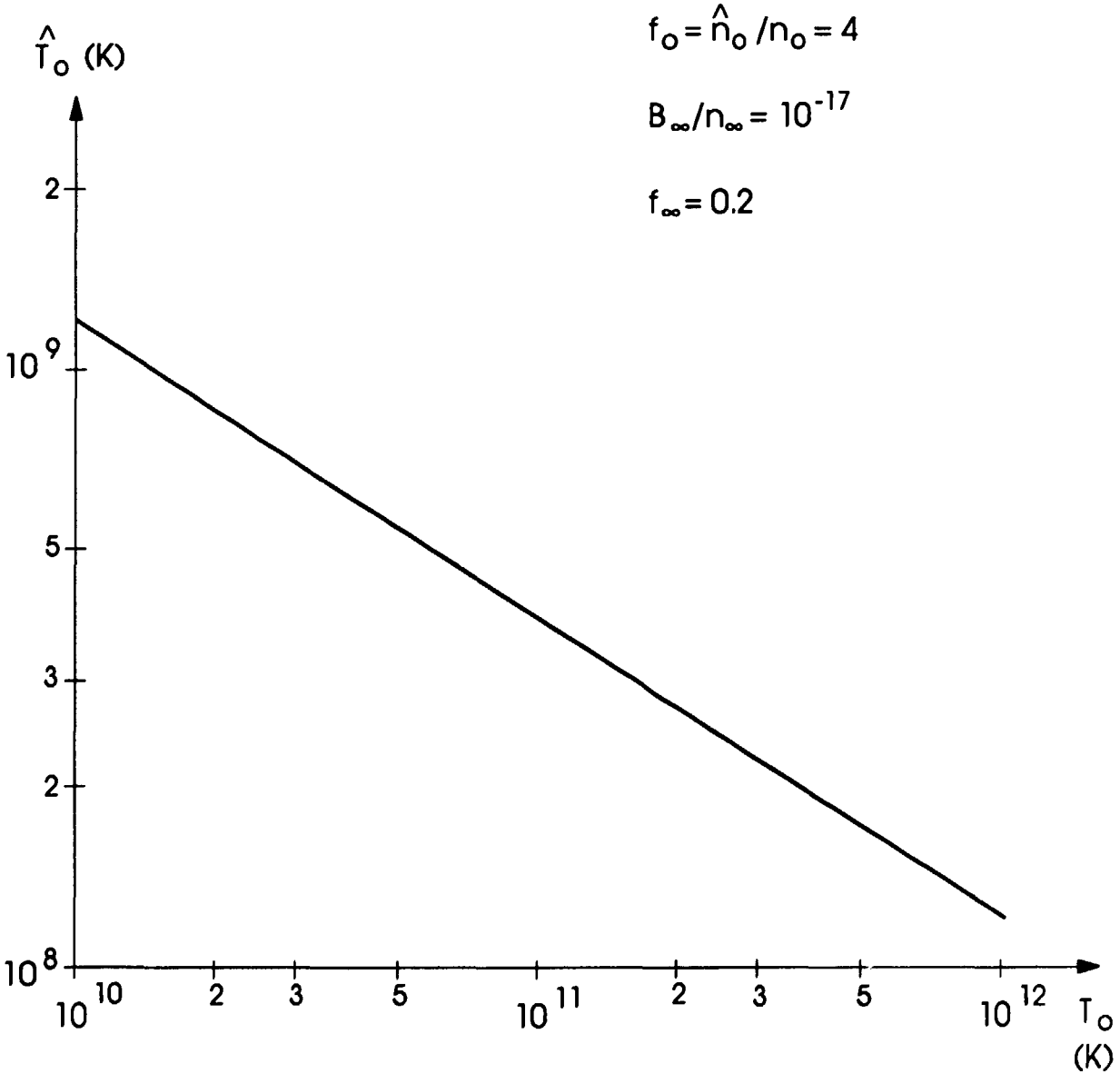
$\hat{T}_o$ (K)
$f_o = \hat{n}_o / n_o = 4$
$B_\infty / n_\infty = 10^{-17}$
$f_\infty = 0.2$
2
$10^9$
5
3
2
$10^8$
$10^{10}$
2
3
5
$10^{11}$
2
3
5
$10^{12}$
$T_o$
(K)

Fig. 5

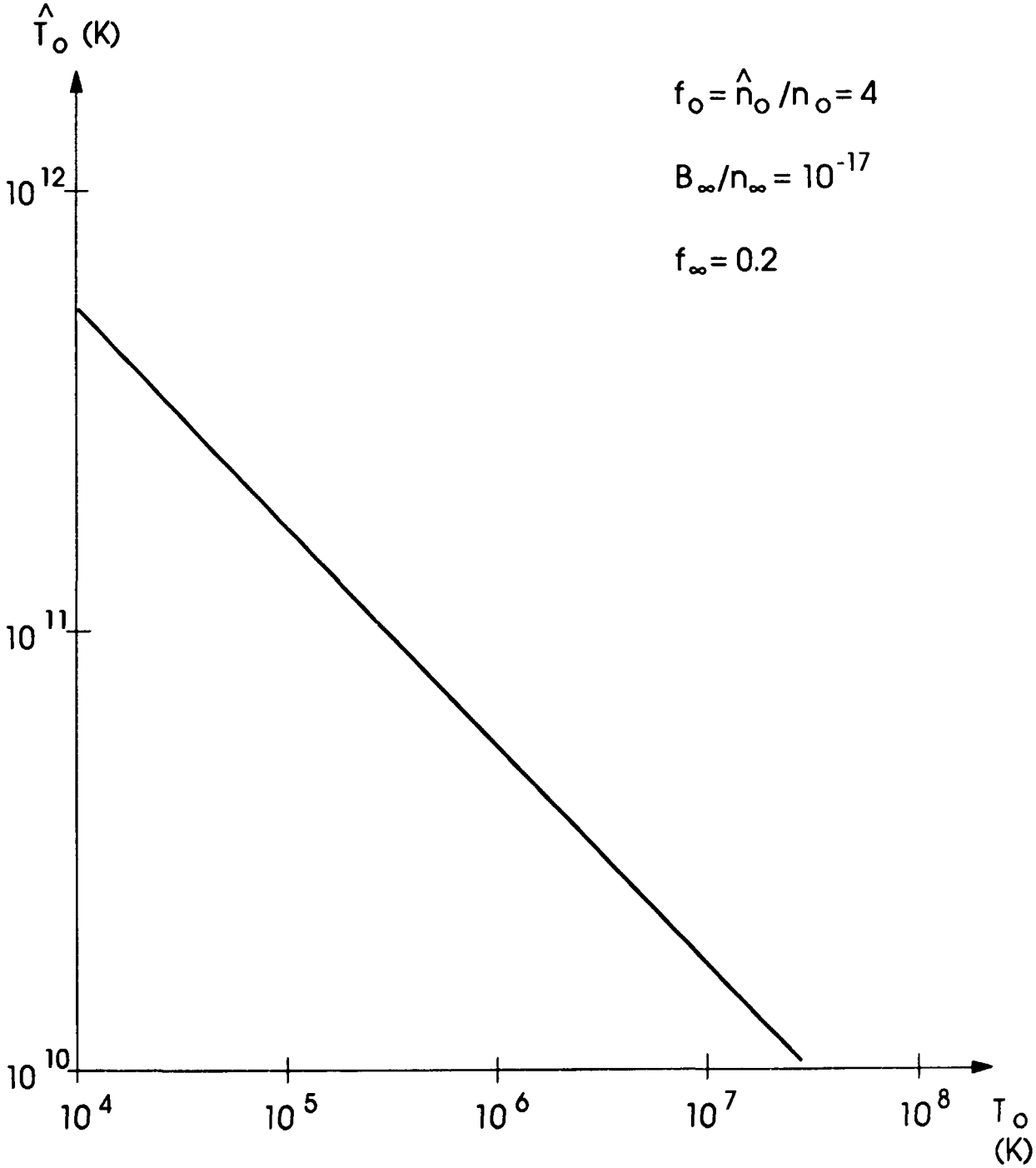
$\hat{T}_o$ (K)
$f_o = \hat{n}_o / n_o = 4$
$B_\infty / n_\infty = 10^{-17}$
$f_\infty = 0.2$
$10^{12}$
$10^{11}$
$10^{10}$
$10^4$
$10^5$
$10^6$
$10^7$
$10^8$
$T_o$ (K)

Fig. 6

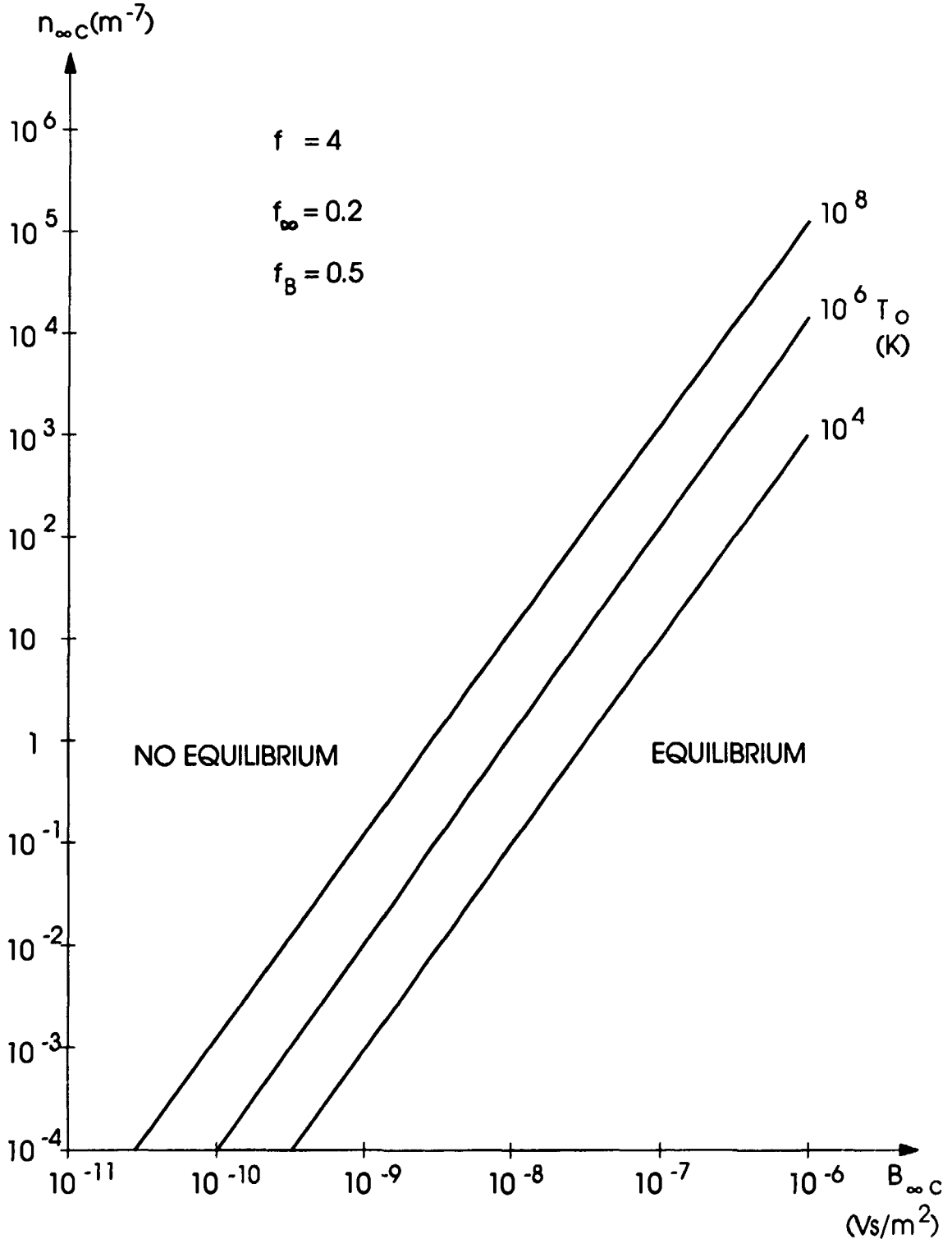
$n_{\infty C}(m^{-7})$
$10^{6}$
$10^{5}$
$10^{4}$
$10^{3}$
$10^{2}$
10
1
$10^{-1}$
$10^{-2}$
$10^{-3}$
$10^{-4}$
f = 4
$f_{\infty} = 0.2$
$f_B = 0.5$
$10^{8}$
$10^{6}$ $T_O$ (K)
$10^{4}$
NO EQUILIBRIUM
EQUILIBRIUM
$10^{-11}$
$10^{-10}$
$10^{-9}$
$10^{-8}$
$10^{-7}$
$10^{-6}$
$B_{\infty C}$ ($Vs/m^2$)

TRITA-EPP-90-04

Royal Institute of Technology, Department of Plasma Physics and Fusion Research, Stockholm, Sweden

# COMPLEMENTARY ASPECTS ON MATTER-ANTIMATTER BOUNDARY LAYERS

B. Lehnert, May 1990, 23 p. in English

This paper gives some complementary aspects on the problems of the matter-antimatter metagalaxy model and its cellular structure, as being proposed by Klein and Alfvén.

A previously outlined one-dimensional model of a magnetized matter-antimatter boundary layer is updated and extended, by introducing amended nuclear annihilation data, and by making improved approximations of the layer structure and its dependence on relevant parameters.

The critical beta value obtained from this model leads to critical plasma densities which are not high enough to become reconcilable with a cellular matter-antimatter structure within the volume of a galaxy. Additional investigations are required on the questions whether the obtained beta limit would still apply to cells of the size of a galaxy, and whether large modifications of this limit could result from further refinements of the theory and from the transition to a three-dimensional model.

Attention is called to the wide area of further research on ambiplasma physics, and on a three-dimensional cell structure with associated problems of equilibrium and stability. In particular, the high-energy ambiplasma component has to be further analysed in terms of kinetic theory, on account of the large Larmor radii of the corresponding electrons and positrons.

Key words: Ambiplasma universe, annihilation reactions, cellular structure, magnetic confinement, ambiplasma stability.